Advances in Engineering Research, volume 213
Proceedings of the International Scientific and Practical Conference "Young Engineers of the Fuel and Energy Complex: Developing the Energy Agenda of the Future" (EAF 2021)

Study of Damping Regulators Unloading in the Virtual Synchronous Generator Method

Ruslan Migranov[1,*] Nikita Dobroskok[1] Anton Morozov[2]

[1]*Department of Automatic Control Systems, Saint Petersburg Electrotechnical University "LETI", St. Petersburg, Russia*
[2] *RePack AS, Oslo, Norway*
[*]*Corresponding author. Email: rmmigranov@stud.etu.ru*

ABSTRACT
Modern trends are leading to an increase in the number of alternative and renewable DC power sources, which are switched on in parallel operation with the main power source, which is a synchronous generator (SG) or a powerful AC network, through a semiconductor autonomous voltage inverter. In order to provide conditions of their synchronization and further long-term stable joint operation the method of virtual SG (VSG), which allows the inverter to imitate static and dynamic properties of the real SG, has been developed. The paper presents a description and structure of microgrid in which the problem of damping controllers of the output voltage parameters controls system of a three-phase bridge voltage source invertor (TBVSI) is investigated to improve the quality of synchronization. The results of modelling allow to give recommendations for controllers unloading technique, which ensures the absence of overshooting of active and reactive power components of the inverter and SG at the moment of synchronization.

Keywords: *Synchronous generator, Microgrid, Inverter, Virtual synchronous generator, Damping regulator, Three-phase bridge voltage source invertor.*

1. INTRODUCTION

At present, an actual direction of energy development is the introduction of alternative and renewable energy sources, such as wind generators, solar panels, or energy storage (batteries) into the power supply system. In order to integrate them it is necessary to use DC to AC converters, for which TBVSI is widely used in three-phase networks [1]. Since TBVSI, unlike AC SGs which are the main power sources in networks, is a static power converter, the known theory cannot be applied to synchronize multiple SGs. In addition, when they work together, a situation arises where two voltage sources with significantly different dynamic and static properties operate on the same load, which worsens the stability of the system. Therefore, the researchers proposed a way for the inverter to imitate the static and dynamic properties of SGs, this approach is called VSG. There are various ways and modifications of this method, but in all of them, the inverter amplitude and phase control equations are based on the swing equation for the real SG represented in relation to the mechanical powers. The basic version of algorithm is described in [2]; in order to increase the accuracy of regulation the internal circuits of output current and voltage of TBVSI are used [3–12]; besides, when TBVSI is supplied from accumulator battery, the primary source voltage regulator is considered [13–15], but for this work VSG with pre-synchronization considered in [16–23] is of particular interest. Apart from VSG, there are also induction motor method [24], approaches with different modifications of phase locked loop (PLL) [25], synchronverters [26] and many others.

The purpose of this paper is to investigate in more detail the operation of damping regulators in controlling the output voltage amplitude and phase of TBVSI, namely, the processes of smooth unloading of output values of regulators when they are switched off to avoid overshoot in calculating the active and reactive power components of the inverter and SG at the moment of synchronization.

In this paper, the control system of TBVSI based on the method of VSG with pre-synchronization is considered and described, as well as the process of damping regulators unloading and its influence on the

transient process of inverter power after synchronization is investigated.

2. THE BASIC VSG METHOD WITH MODIFICATIONS AND THE ROLE OF THE DAMPING REGULATOR UNLOADING

2.1. Inverter output voltage amplitude and phase control system of VSG methods

Among the many variations of the VSG method, some take the output voltage amplitude and phase mismatch into account [16–18] and some do not [4–6]. There is also a variation of modifications that improve the pre-synchronization process, for example, by introducing an integrating additive component in the damping regulator that allows one to avoid the static error in the calculation of the amplitude and phase that occurs in the basic VSG method. Therefore, here is the swing equation for SG:

$$J \cdot \frac{d\omega}{dt} = T_m - T_e - T_{damp} \quad (1)$$

where J is the moment of inertia; T_m, T_e are mechanical and electromagnetic moments; T_{damp} is the damping moment equivalent to the friction force moment in the SG.

Since the TBVSI is a static inverter and Newton's second law of motion does not apply to it, let us rewrite the right-hand side of Equation (1) through powers by multiplying the torque value by the rated (desired) frequency of the inverter output voltage ω_n [16]

$$J \cdot \omega_n \cdot \frac{d\omega}{dt} = P_m - P_e - P_{damp}$$

where $J \cdot \omega_n = J_{VSG}$ is the virtual moment of inertia of the VSG, determining the inertial properties of the SG; P_m and P_e are mechanical and electromagnetic power; P_{damp} is the damping power, determined according to the expression:

$$P_{damp} = \begin{cases} D_P \cdot (\omega_n - \omega), & \text{trad.} \\ (D_P + \dfrac{K_{PI}}{s}) \cdot (\omega_n - \omega), & \text{trad. with mods} \end{cases}$$

where D_p and K_{PI} are the proportional and integrating coefficients of the damping regulator.

As mentioned earlier, the VSG is based on the imitation of the static and dynamic properties of the SG, so the inverter output voltage frequency equation ω is based on the generator swing equation.

The rotor speed droop controller in the generator must also be taken into account, so the mechanical power will be of the form:

$$P_m = P_n - k_p \cdot (\omega_n - \omega)$$

where P_n is the specified (desired) active power; k_p is the frequency droop factor.

With this in mind, an equation describing the frequency of the inverter output voltage is obtained:

$$J_{VSG} \frac{d\omega}{dt} = P_n - P_e - \begin{cases} K_P \cdot (\omega_n - \omega), & \text{trad.} \\ (K_P + \dfrac{K_{PI}}{s}) \cdot (\omega_n - \omega), & \text{mod.} \end{cases} \quad (2)$$

where $K_p = D_p + k_p$ is the resulting proportional component ratio of the damping regulator.

Equation (2) can be presented in relation to the difference between the desired and estimated frequency value $\Delta\omega = \omega_n - \omega$, so it can be safely assumed:

$$\frac{d\omega}{dt} = \frac{d(\omega_n - \omega)}{dt} = \frac{d\Delta\omega}{dt} \quad (3)$$

Now moving into the operational domain, with the Laplace operator s.

$$(J_{VSG} \cdot \Delta\omega) \cdot s = P_n - P_e - \begin{cases} K_P \cdot \Delta\omega, & \text{trad.} \\ (K_P + \dfrac{K_{PI}}{s}) \cdot \Delta\omega, & \text{mod.} \end{cases} \quad (4)$$

The phase of the inverter output voltage will be obtained by integrating the voltage frequency value:

$$\theta = \frac{1}{s} \cdot (\omega_n + \Delta\omega)$$

Equation (4) is better represented as a block diagram, as shown in Figure 1. Similarly, the output voltage amplitude of the inverter is calculated as [16, 18]:

$$K \cdot \frac{dU_n}{dt} = Q_n - Q_e - Q_{damp} \quad (5)$$

where Q_n, Q_e and Q_{damp} are specified (desired), electromagnetic and damping reactive power of the inverter; U_n is the desired output voltage amplitude; K is the virtual voltage coefficient.

The damping reactive power can be defined as:

$$Q_{damp} = \begin{cases} D_Q \cdot (U_n - U), & \text{trad.} \\ (D_Q + \dfrac{D_{QI}}{s}) \cdot (U_n - U), & \text{mod.} \end{cases}$$

where D_Q and D_{QI} are the proportional and integrating coefficients of the damping regulator.

Similar to (3) and (4), the difference in amplitude ΔU can also be represented, then (5) will be:

$$(K \cdot \Delta U) \cdot s = Q_n - Q_e - \begin{cases} D_q \cdot \Delta U, & \text{trad.} \\ (D_q + \dfrac{D_{qI}}{s}) \cdot \Delta U, & \text{mod.} \end{cases} \quad (6)$$

Also, for a better representation of (6), plot its structural diagram in Figure 1.

The damping regulators are deactivated with the switches SW1 and SW2. As a result, after switching off the damping regulators (4) and (6) will look like:

$$(J_{VSG} \cdot \Delta\omega) \cdot s = P_n - P_e$$
$$(K \cdot \Delta U) \cdot s = Q_n - Q_e$$

Therefore, if the desired power value is changed after turning off the regulators, the estimated and desired power values will be equal after the completion of the transients. For this reason, the timing and method of switching off the regulators is of particular interest.

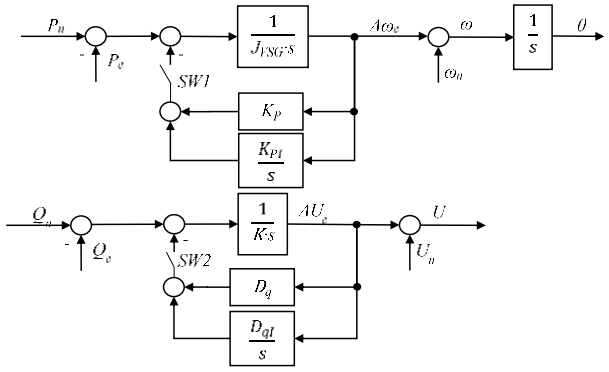

Figure 1. Diagram of inverter output voltage amplitude and phase control

Among the presented system parameters, the damping controller's integration factor (K_{PI}, D_{QI}) and frequency droop factor k_p are empirically found. Let's calculate the remaining ones according to [2, 18].

The proportional component of the damping regulators is determined by the *P*-ω and *Q*-*U* characteristics of the SG. The first characteristic is taken at a nominal value of voltage of excitation winding of the generator, and the second at a constant nominal speed of rotation of the rotor. After plotting the characteristics, the range of variation of the corresponding power is set and the diagram to determine the amount of variation of a particular parameter (ω or *U*) is used. The formulas for determining the coefficients are as follows:

$$D_P = \frac{\Delta P}{\Delta\omega \cdot \omega_{set}}, \qquad D_Q = \frac{\Delta Q}{\Delta U},$$

where ΔP and ΔQ are differences in active and reactive powers, Δω and ΔU are differences in rotor speed and field winding voltage.

In contrast to [2], the maximum amplitude and frequency rating of the output voltage in the active power loop is not taken out, so the resulting D_p value must be multiplied by ωn, and D_q by √2.

Also, according to [2] calculate the virtual voltage factor *K*:

$$K \le \frac{5D_q}{\omega_n}$$

The last parameter to be calculated is the virtual moment of inertia, which is determined from the equation [18]:

$$\frac{J_{SG}}{S_{SG}} = \frac{J_{VSG}}{S_{INV}},$$

where J_{SG} and S_{SG} are the moment of inertia and full power rating of the SG, S_{INV} is the full inverter power.

2.2. Synchronization conditions and method of damping regulators unloading

After describing the entire control system for the phase and amplitude of the TBVSI output voltage, let us examine the synchronization conditions and the proposed method of unloading the damping regulator.

In the investigated system we will use the exact synchronization method, setting the values (criteria) [27] for the difference of frequency, phase and amplitude of SG and TBVSI, where for the phase, according to [16] the following is calculated:

$$\omega_{SG} - \omega_{INV} \le \alpha_\omega$$
$$U_{SG} - U_{INV} \le \alpha_U \quad (7)$$
$$1 - \cos(\theta_{SG} - \theta_{INV}) \le \alpha_\theta$$

The choice of criteria depends on the task at hand and the desired synchronization time, since simulation results show that the synchronization time is significantly affected by moments of phase coincidence, which recur periodically, in contrast to the difference between amplitude and frequency, which fluctuates around a stable value over time.

Let us now consider unloading the values accumulated at the output of the damping regulators. This process can be most easily implemented using the exponential law (in the operational domain it takes the form of a real differential), but it should be remembered that the exponent is only zeroed out at infinite time, which can create a static error in the calculations. To avoid this, we force zero the value at the controller output after a time equal to 6τ, at which a rapid jump in the value will not lead to a significant effect on the transient process in the system. Let us give an equation and an implementation of the algorithm for damping regulators unloading, where y_0 is the value at the

controller output at the moment of tripping; t_0 is the tripping time; τ is the time constant of unloading.

$$y = y_0 \cdot e^{-\frac{t-t_0}{\tau}}.$$

Figure 2 (a) represents an implementation of the controller unloading subsystem in Matlab&Simulink software, which is installed in place of switches SW1 and SW2, as shown in Figure 1.

Similarly, it is possible to unload using the following expression:

$$y = y_0 - (t-t_0)^n \cdot \tau \quad (8)$$

where n is a natural number. The signal from the regulators and the cut-off signal must be fed to the input, and the time constant must also be set. The programming code contained in the Function block corresponds to the controller unloading described earlier.

3. MODELLING RESULTS

3.1. Description of the modelled system in Matlab&Simulink

In the paper researches are conducted on an example of system of microgrid, in which as the basic generating installation SG of 85 kW and the rated RMS linear value of output voltage in 400 V which works some time on an active-inductive load, consuming 40 kW of active and 30 kVAR of reactive power serves as the main generating installation. The system provides for possibility of connection for joint operation with SG of direct current source, which by means of TBVSI and after observance of all conditions of synchronization (7) is switched on in parallel operation. At the same time the output voltage of TBVSI is smoothed by a two cascaded LC filter, and its amplitude and phase are regulated by the basic method of VSG with modifications, the structural diagram of the system of which is presented earlier in figure 1. The system parameters are given in Table 1.

Table 1. Coefficient values used in modelling

Parameters	Values	Parameters	Values
J_{VSG}, kg·m^2	0.6296	K	113
K_p	256*2π*50	D_q	5044*√2
K_{PI}	25000	D_{qI}	25000
P_n, W	40000	Q_n, VAR	30000
ω_n, rad/s	2π*50	U_n, V	400*√2/√3
α_ω	0.1	α_θ	1e-10
α_U	0.2	K_{norm}	437.2/400

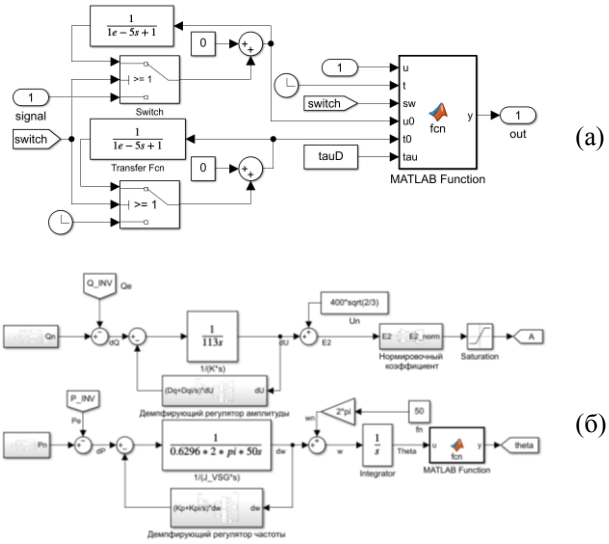

Figure 2 Damping regulator value unloading subsystems (a) and inverter output voltage amplitude and phase control systems (b).

Figure 2 (b) shows the TBVSI output voltage phase and amplitude control system designed in Matlab&Simulink software, based on the block diagrams shown earlier in Figure 1.

The following blocks, not previously included in the system description, should be noted, which are:

- Saturation block – designed to limit the calculated amplitude within the sawtooth signal amplitude, which is used to obtain a pulse width modulated signal;
- Subsystem of amplitude normalization – in this subsystem, after the moment of synchronization, the normalization factor Knorm changes, because at the beginning the inverter operates at idle and the smoothing filter acts as a load, which leads to a distortion of the amplitude value at the inverter output;
- Function block – designed to convert the phase signal into a sawtooth form, taking values from 0 to 2π. The code in this block is also quite primitive and consists of a single while cycle.

3.2. Influence of time constants

Figure 3 shows the diagrams of the inverter power components when changing the unload time constants of the proportional and integrating components of the damping controller.

Figure 3 shows that a larger time constant results in longer control times, while a smaller time constant results in higher overshoot.

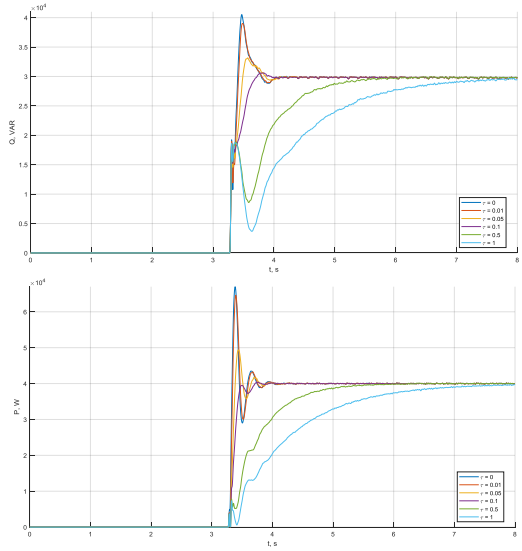

(а)

(б)

Figure 3 Time diagrams of the active and reactive power components of the TBVSI at different values of the damping regulator unloading time constant.

Depending on the application, it is therefore possible to select an unloading time constant at which all conditions are met. In this case, for the absence of overshoot, it is sufficient to select an unloading time constant of 0.5s for both components of the damping controller. Also from Figure 3, it can be seen that it is possible to find evidence of the fact that there is no overshoot. 3, it can be confirmed that after switching off the regulators, the power distribution takes place without any static error.

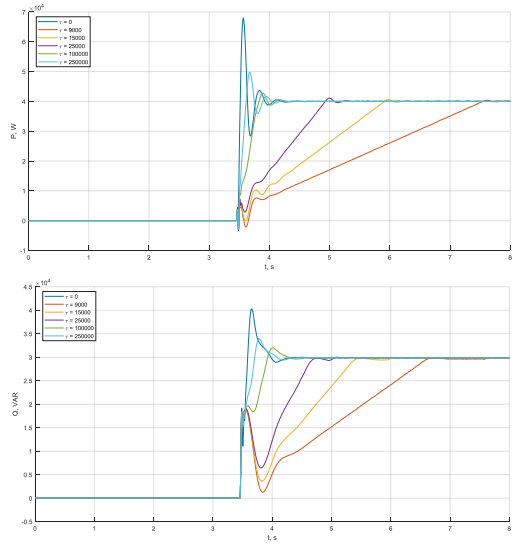

(а)

(б)

Figure 4 Time diagrams of the active and reactive power components of the TBVSI when the regulator is linearly unloaded/

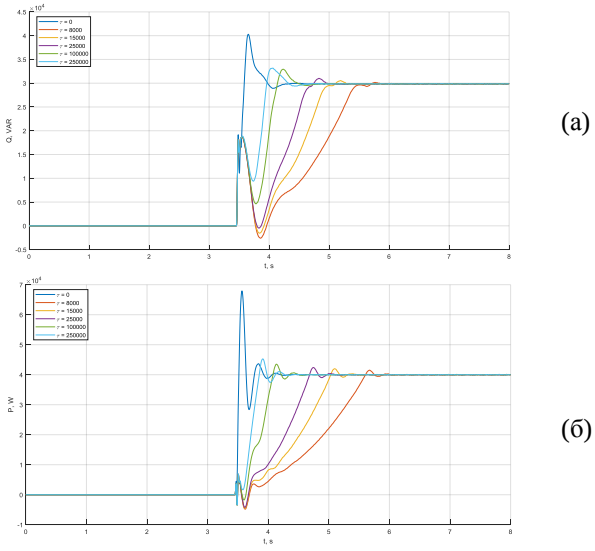

(а)

(б)

Figure 5 Time diagrams of the active and reactive power components of the TBVSI with quadratic controller unloading.

Figure 4 shows the diagrams of the power components of the inverter. Figure 4 shows diagrams of inverter power components at linear unloading according to (8), from which it can be seen that even at the slowest unloading, there is a small jump in power values at the moment of complete zeroing. The derived quantitative transient parameters such as the control and overshoot time for each type of unloading are given in Table 2.

Figure. 5, which shows the quadratic unloading of the regulators, compared to the linear unloading has a larger oscillation at full zeroing, but a shorter regulation time.

Table 2. Modelling results

Type of unload	Parameters	Discharge factor value				
		τ_1	τ_2	τ_3	τ_4	τ_5
Exponential	Active power P_{INV}					
	t_p, s	3,93	3,98	4,02	5,68	7,99
	σ, %	62,5	22,5	1	0	0
	Reactive power Q_{INV}					
	t_p, s	3,77	3,82	3,97	5,82	7,87
	σ, %	30	10	2	0	0
Linear	Active power P_{INV}					
	t_p, s	3,86	4,04	4,98	5,95	7,6
	σ, %	22,5	6,75	2,5	1,5	1
	Reactive power Q_{INV}					
	t_p, s	4,2	4,36	4,76	5,49	6,72
	σ, %	13.3	6.6	0	0	0
Quadratic	Active power P_{INV}					
	t_p, s	4,23	4,4	4,8	5,16	5,73
	σ, %	13,25	8,5	6	5	3,75
	Reactive power Q_{INV}					
	t_p, s	4,27	4,4	4,7	5,03	5,6
	σ, %	10,66	10	3	1,66	0,67

4. CONCLUSION

As a result of this paper, studies have been carried out on the example of an microgrid system in which, in parallel with the SG, a DC source is connected via a TBVSI controlled by the VSG method with modifications. Special attention was paid to the damping regulators part of the control system with phase and inverter amplitude control in terms of their gradual switching off.

With the results of the study, it can be concluded that by unloading the accumulated values at the output of the damping regulators according to the exponential law, the control time of the transient increases at high time constants and the oscillation at low constants.

By comparing all three unloading types, it can be concluded that exponential unloading is the most desirable, because using a linear or quadratic law has a negative effect on the transient of the power components of the inverter and introduces oscillation, with large time constants.

This study is intended to facilitate the synthesis of inverter output voltage parameter control systems using the VSG method. For small tables, please place it within a column and bigger table be placed in a text frame spanning to both columns. Use the Table facility available within the MSWord. The font in the row header should be bold and you can use the style available from the style palette.

AUTHORS' CONTRIBUTIONS

Ruslan Migranov: Corresponding author, performed research, lead author, co-analyzed data. Nikita Dobroskok: analyzed data, mathematical modelling, co-authors. Anton Morozov: performed research, analyzed results, co-authors.

REFERENCES

[1] Migranov R.M. Inverter Power Generation Control in Microgrid: Bachelor's thesis – ETU "LETI", 2021, 79 p. URL: https://nauchkor.ru/pubs/upravlenie-invertornoy-generatsiey-energii-v-sisteme-maloy-raspredelennoy-energetiki-60eacc83e4dde500016d320b

[2] Hao, Yue & Li, Hua. (2020). Research on VSG Control Strategy of Microgrid. IOP Conference Series: Earth and Environmental Science. 440. 032087. 10.1088/1755-1315/440/3/032087.

[3] A. Tuckey and S. Round, "Practical application of a complete virtual synchronous generator control method for microgrid and grid-edge applications," 2018 IEEE 19th Workshop on Control and Modeling for Power Electronics (COMPEL), 2018, pp. 1-6, DOI: 10.1109/COMPEL.2018.8459987.

[4] Wang, Yawei & Liu, Bangyin & Duan, Shanxu. (2019). A Modified Virtual Inertia Control Method of VSG Strategy with Improved Transient Response and Power Supporting Capability. IET Power Electronics. 12. 10.1049/iet-pel.2019.0099.

[5] Y. Wang, B. Liu and S. Duan, "Improving Transient Response of VSG Controlled Grid-Tied Converter," 2019 IEEE Applied Power Electronics Conference and Exposition (APEC), 2019, pp. 1825-1828, DOI: 10.1109/APEC.2019.8722266.

[6] X. Zheng, Y. Liu, S. Pang, Z. Liu, Y. Li and C. Wang, "Sliding Mode combined VSG Control to Microgrid Inverters," IECON 2018 - 44th Annual Conference of the IEEE Industrial Electronics Society, 2018, pp. 2453-2456, DOI: 10.1109/IECON.2018.8592771.

[7] Hou, Xiaochao & Sun, Yao & Zhang, Xin & Lu, Jinghang & Wang, Peng & Guerrero, Josep. (2019). Improvement of Frequency Regulation in VSG-Based AC Microgrid Via Adaptive Virtual Inertia. IEEE Transactions on Power Electronics. Pp. 1-1. 10.1109/TPEL.2019.2923734.

[8] Xu, Y.; Nian, H.; Wang, Y.; Sun, D. Impedance Modeling and Stability Analysis of VSG Controlled Grid-Connected Converters with Cascaded Inner Control Loop. Energies 2020, 13, 5114. https://doi.org/10.3390/en13195114

[9] Volkov A. & Sagaiko D. (2020). A research into the operation of a system of electric energy accumulation as part of a cyber-physical real time simulation facility. Power and Autonomous equipment. 2. 209-218. 10.32464/2618-8716-2019-2-4-209-218.

[10] W. Jian, L. Tong, L. ZiDong and X. DianGuo, "VSG Current Balance Control Strategy Under Unbalanced Grid Voltage," 2019 22nd International Conference on Electrical Machines and Systems (ICEMS), 2019, pp. 1-6, DOI: 10.1109/ICEMS.2019.8922266.

[11] C. Wang, J. Wu, D. Yang and J. Zhao, "Suppressing power oscillation based on VSG," 2017 IEEE 2nd Information Technology, Networking, Electronic and Automation Control Conference (ITNEC), 2017, pp. 336-339, DOI: 10.1109/ITNEC.2017.8285001.

[12] Zhang, B.; Yan, X.; Li, D.; Zhang, X.; Han, J.; Xiao, X. Stable Operation and Small-Signal Analysis of Multiple Parallel DG Inverters Based on a Virtual Synchronous Generator Scheme.

Energies 2018, 11, 203. https://doi.org/10.3390/en11010203

[13] V. S. K. M. Balijepalli, A. Ukil, N. Karthikeyan, A.K. Gupta and Y. Shicong, "Virtual synchronous generators as potential solution for electricity Grid compliance studies," 2016 IEEE Region 10 Conference (TENCON), 2016, pp. 718-722, DOI: 10.1109/TENCON.2016.7848096.

[14] Ding, Xiying, Tianxiang Lan, and Henan Dong. "Control Strategy and Stability Analysis of Virtual Synchronous Generators Combined with Photovoltaic Dynamic Characteristics." Journal of Power Electronics 19, no. 5 (September 20, 2019): 1270–77. DOI:10.6113/JPE.2019.19.5.1270.

[15] W. Gao, "Microgrid Control Strategy Based on Battery Energy Storage System-Virtual Synchronous Generator (BESS-VSG)," 2020 IEEE Kansas Power and Energy Conference (KPEC), 2020, pp. 1-6, DOI: 10.1109/KPEC47870.2020.9167653.

[16] Chen, Xuhai & Zhang, Yiwang & Dong, Jiqing & Mao, Xingkui & Chen, Jiaqiao & Wen, Buyin & Zhang, Zhe. (2020). A Novel Pre-Synchronization Control for Grid Connection of Virtual Synchronous Generator. Elektronika ir Elektrotechnika. 26. 25-31. 10.5755/j01.eie.26.6.25874.

[17] Yu, Yong-jin & Cao, Li-ke & Zhao, Xingmin. (2018). A novel control strategy of virtual synchronous generator in island micro-grids. Systems Science & Control Engineering. 6. 136-145. 10.1080/21642583.2018.1539930.

[18] K. Shi, W. Song, H. Ge, P. Xu, Y. Yang and F. Blaabjerg, "Transient Analysis of Microgrids With Parallel Synchronous Generators and Virtual Synchronous Generators," in IEEE Transactions on Energy Conversion, vol. 35, no. 1, pp. 95-105, March 2020, DOI: 10.1109/TEC.2019.2943888.

[19] J. Wu, F. Zhuo, Z. Wang, H. Yi and K. Yu, "Pre-synchronization method for grid-connection of virtual synchronous generators based micro-grids," 2017 19th European Conference on Power Electronics and Applications (EPE'17 ECCE Europe), 2017, pp. P.1-P.8, DOI: 10.23919/EPE17ECCEEurope.2017.8099309.

[20] P. Xing, X. Jia, C. Tian, Y. Mao, L. Yu and X. Jiang, "Pre-synchronization Control Method of Virtual Synchronous Generator with Alterable Inertia," 2019 IEEE 10th International Symposium on Power Electronics for Distributed Generation Systems (PEDG), 2019, pp. 142-146, DOI: 10.1109/PEDG.2019.8807766.

[21] Zhou, Zifu & Long, Jun. (2020). An improved grid-connected pre-synchronization method for photovoltaic micro-grid. Journal of Physics: Conference Series. 1549. 052040. 10.1088/1742-6596/1549/5/052040.

[22] Zhang, H. & Zhang, R. & Sun, K. & Feng, W. (2019). Performance improvement strategy for parallel-operated virtual synchronous generators in microgrids. Journal of Power Electronics. 19. 580-590. 10.6113/JPE.2019.19.2.580.

[23] X. Li and G. Chen, "Synchronization Strategy for Virtual Synchronous Generator based Energy Storage System," IECON 2019 – 45th Annual Conference of the IEEE Industrial Electronics Society, 2019, pp. 2512-2517, DOI: 10.1109/IECON.2019.8927372.

[24] M. Ashabani, F. D. Freijedo, S. Golestan and J. M. Guerrero, "Inducverters: PLL-Less Converters With Auto-Synchronization and Emulated Inertia Capability," in IEEE Transactions on Smart Grid, vol. 7, no. 3, pp. 1660-1674, May 2016, DOI: 10.1109/TSG.2015.2468600.

[25] Jackson, Ronald & Aizam, Shamsul & Benbouzid, Mohamed & Salimin, Suriana & Khan, Mubashir & Garba, Elhassan & Pathan, Erum. (2020). A Comprehensive Motivation of Multilayer Control Levels for Microgrids: Synchronization, Voltage and Frequency Restoration Perspective. Applied Sciences. 10. 8355. 10.3390/app10238355.

[26] G.P. da Silva Junior and L.S. Barros, "Synchronverter Operation in Active and Reactive Support Mode," 2019 Workshop on Communication Networks and Power Systems (WCNPS), 2019, pp. 1-5, DOI: 10.1109/WCNPS.2019.8896239.

[27] Guanfeng Zhang, Junyou Yang, Haixin Wang, Jia Cui, "Presynchronous Grid-Connection Strategy of Virtual Synchronous Generator Based on Virtual Impedance", Mathematical Problems in Engineering, vol. 2020, Article ID 3690564, 9 pages, 2020. https://doi.org/10.1155/2020/3690564